RSC Advances

PAPER

View Article Online
View Journal | View Issue

Cite this: *RSC Adv.*, 2022, **12**, 3969

Structure and properties of chitosan/sodium dodecyl sulfate composite films†

Song Jiang, Congde Qiao,* Xujie Wang, Zhongwei Li* and Guihua Yang

Received 9th November 2021
Accepted 24th January 2022

DOI: 10.1039/d1ra08218c

rsc.li/rsc-advances

In this study, we investigated the effect of sodium dodecyl sulfate (SDS) content on the structure and properties of chitosan films. It is found that the binding of SDS to chitosan was realized through the interactions between $-SO_4^-$ and $-NH_3^+$, forming an ionically cross-linked film. Structural analysis revealed that the crystallization was greatly hindered by introducing SDS. With an increase of SDS content, the glass transition temperatures (T_g) of chitosan films increased due to the formation of crosslinks. Compared to pure chitosan film, the composite films had lower content of moisture and possessed better thermal stability. In addition, the mechanical properties of the as-obtained composite films were closely related to the content of SDS, and were significantly improved in the biopolymer films with moderate SDS content. These results indicate that the microstructure as well as properties of the chitosan films can be regulated by adding SDS.

1. Introduction

Chitosan is one of the most important cationic biopolymers produced from the partial or complete deacetylation of chitin. It has many potential applications in the food industry, cosmetics, medicine and environmental protection.[1] In addition, chitosan is particularly suitable to be used as a packaging material because of its good film-forming properties.[2] However, this biopolymer film is relatively brittle and fragile, and its application is limited due to the poor mechanical properties as well as high hygroscopicity.[3]

To overcome this issue, modification studies have been conducted to improve the properties of chitosan films.[4] Compared to covalent modification, non-covalent modification of chitosan is extremely attractive due to avoiding of the tedious synthesis and potentially environmental issues. Generally, the flexibility of chitosan film can be improved by the addition of plasticizers because of the disruption of the hydrogen bonding between biopolymer molecules. Nevertheless, the mechanical strength of biopolymer film was generally weakened due to an increase in the chain flexibility.[5] Therefore, how to simultaneously improve both strength and flexibility of biopolymer film still remains a critical challenge.

In addition to hydrogen bonds, electrostatic and hydrophobic interactions also exist in chitosan system.[6–8] It is expected that changes in these interactions will directly or indirectly interfere in structure formation and result in the variation of biopolymer properties. As a cationic polyelectrolyte, chitosan is prone to interact with anionic surfactants through electrostatic attraction as well as hydrophobic interaction.[9] It has been demonstrated that many of the properties of chitosan depend on its ability to interact with anionic surfactant molecules.[10] As sodium dodecyl sulfate (SDS) is a well characterized anionic surfactant, and chitosan/SDS system has been studied extensively as a model polyelectrolyte-surfactant system that exhibits different physiochemical properties. For instance, Chatterjee and co-workers reported that the dye adsorption properties of chitosan-based hydrogel capsules were closely related to the content of SDS.[11] Moreover, it showed that the adsorption capacity of Cr(VI) on chitosan–SDS beads varied with initial concentrations of SDS.[12] Similar results were also observed for the adsorption of malachite green and congo red on chitosan–SDS beads.[13,14] Very recently, Bandforuzi and Hadjmohammadi prepared a special kind of SDS-coated magnetic chitosan nanoparticles, and found that these nanoparticles had a high adsorption capacity of organophosphorus pesticides due to the strong interactions between sorbent and target analytes.[15] In addition, the presence of SDS could significantly increase the hydrophobicity and interfacial activity of chitosan, and endow chitosan–SDS complexes with a remarkably emulsifying ability.[16]

Many applications of chitosan depend on the interactions between polyelectrolyte and oppositely charged surfactant.[17] The binding behaviors of SDS to chitosan in solutions have been studied widely.[9,10,18] It was generally observed that SDS bound strongly to chitosan through electrostatic interactions evidenced by a distinct exothermic valley at low surfactant concentration, whereas a broad endothermic plateau appeared

School of Materials Science and Engineering, State Key Laboratory of Biobased Material and Green Papermaking, Qilu University of Technology (Shandong Academy of Sciences), Daxue Rd. 3501, Jinan 250353, PR China. E-mail: cdqiao@qlu.edu.cn; lizhw2007@126.com; Fax: +86 531 89631227; Tel: +86 531 89631227

† Electronic supplementary information (ESI) available. See DOI: 10.1039/d1ra08218c

at high SDS content, indicating that some weak hydrophobic interaction occurred between polymer and surfactant.[18–20] In addition, the chitosan–SDS interactions at a solid–liquid interface was investigated and it was found that the binding behaviors in bulk and at solid–liquid interfaces were rather different.[21,22] Due to its gel-forming properties, chitosan-based system is generally used in solid state, especially in film state. So the study of the interaction of chitosan with SDS in films is important and urgent. Unfortunately, few work has been done on the chitosan–SDS interactions in biopolymer films. He and co-workers[23,24] observed that the chitosan interacted electrostatically with SDS micelles, which acted as network junctions and endowed the chitosan hydrogel films with high mechanical strength. Additionally, it was stated that SDS could bind to the cross-linked chitosan films, and this cooperative binding resulted in the collapse of the polymer gels.[25] So far, however, there still lacks of systematic research on the influence of SDS on the structure and properties of chitosan films.

In this work, the effect of SDS content on the structure and properties of chitosan films was investigated in detail. Importantly, the interactions between chitosan and SDS in the biopolymer films were explored. The aim of this study is to provide a better understanding of the interactions between polyelectrolyte and oppositely charged surfactant. Furthermore, the knowledge of the structure–property relationship of composite films is beneficial for the design and development of biopolymer/surfactant-based products with desirable properties.

2. Experimental

2.1 Materials

Chitosan (degree of deacetylation: 88.7, the viscosity-average molecular weight is about 2.6×10^5, and is determined by the viscosity method, viscosity 100–150 mPa s), glacial acetic acid and sodium dodecyl sulfate were purchased from Sinopharm Chemical Reagent Co., Ltd, China. All aqueous solutions are prepared with ultrapure water (18.25 MΩ), and all the chemical reagents were of analytical grade.

2.2 Preparation of chitosan films

In this work, chitosan films were prepared by solution casting method. First, a certain amount of chitosan powder was dissolved in a 0.2 mol L^{-1} CH_3COOH aqueous solution, stirred overnight to obtain a chitosan solution of 2 wt%. Then, the chitosan solutions were filtered using a PTFE membrane with a pore size of 0.22 μm to remove insoluble impurities. Then, 30 mL of the chitosan solution was cast into a PTFE mold and dried at room temperature for 72 hours. Finally, the obtained chitosan films were placed in a vacuum oven for 24 hours at 70 °C, yielding dry film samples.

2.3 Preparation of chitosan/SDS composite films and conditioning

First, a certain amount of sodium dodecyl sulfate (SDS) powder was dissolved in ultrapure water to prepare a solution with a mass concentration of 0.5, 1, 2, 4, 8, 12, 16, 18, 20 and 25 wt%, respectively. Then, the dried chitosan films were cut into uniform small pieces, and were immersed in SDS solutions with different concentrations at a constant temperature of 25 °C for 24 hours to complete the cross-linking process. Afterwards, the cross-linked films were taken out, rinsed with distilled water to neutrality and dried in a vacuum oven for 24 hours at 70 °C. The obtained dry composite films were conditioned at room temperature (25 °C) in desiccators for at least two weeks at 68.9% relative humidity for further analysis. In this work, the relative humidity is controlled by the saturated aqueous solution of KI. It has been verified that the humidity of the air above the liquid level of the saturated aqueous solution of KI in a closed container is about 68.9%.

2.4 Methods

2.4.1 Scanning electron microscopy (SEM). The surface morphology of the composite films was studied by Geminisem 500 scanning electron microscopy (Carl Zeiss Microscopy GmbH, Germany). The samples were sprayed with gold layer to improve their conductivity and fixed on the sample stub by double-sided tape. The acceleration voltage used in the test is 3 kV.

2.4.2 Fourier-transform infrared (FTIR) spectroscopy. FTIR data for the composite films was obtained by using a Nicolet iS10 spectrometer (Thermo Fisher Scientific Inc., Waltham, MA, USA), equipped with an attenuated total reflection (ATR) accessory. The FTIR spectra were recorded from 400 to 4000 cm^{-1} with a resolution of 4 cm^{-1} and 16 scans. The data were analyzed with an Omnic software.

2.4.3 X-ray diffraction (XRD). XRD patterns of composite films were recorded by an X-ray diffractometer (Bruker D8, Germany) equipped with a multichannel detector by use of a Cu $K\alpha_1$ ($\lambda = 0.1542$ nm) monochromatic X-ray beam. All the specimens were determined in the scattering range of (2θ) 3–50° with a scan rate of $5°min^{-1}$.

2.4.4 X-ray photoelectron spectroscopy (XPS) and element analyzer (EA). X-ray photoelectron spectroscopy (ESCALAB 250Xi, USA) was used to characterize the changes in surface elements of chitosan films after introduction of SDS. In addition, an element analyzer (Vario EL cube, Germany) was used to measure the content of each element in the composite films, and the SDS content was determined by the ratio of N/S elements.

2.4.5 Differential scanning calorimetry (DSC). DSC experiments were performed on a Q 2000 DSC (TA Instrument, New Castle, USA) equipped with a cooling accessory RCS90. All the composite films with mass of ~10 mg were sealed in the Tzero hermetic pans with lids and heated from 20 to 120 °C at a heating rate of 10 °C min^{-1}. All measurements were conducted under nitrogen flow of 50 mL min^{-1}. The experimental data were determined at least by triplicate on each film sample.

2.4.6 Thermogravimetric analysis (TGA). TGA measurements were carried out on a TGA-1 (Mettler Toledo Instrument, Zurich, Switzerland) from 45 to 800 °C under nitrogen

atmosphere at a heating rate of 10 °C min^{-1}. In addition, TGA was also applied to accurately determine the water content of the composite films, and the results were shown in Fig. S1.† The conditioned films were first heated to 110 °C with a heating rate of 10 °C min^{-1}, and then equilibrated at this temperature for 60 min. The water content was determined from the weight loss at the end of the experiment.

2.4.7 Mechanical properties. The mechanical properties of chitosan/SDS composite films were measured using a Universal testing machine (WDL-005, Jinan Xinshiji Experimental Instrument Co., China). The standard method used for measuring the mechanical properties is ASTM D882-18-Standard Test Method for Tensile Properties of Thin Plastic Sheeting. Test strip dimensions were 50 mm × 10 mm (length × width). The tensile experiments were performed at room temperature (25 °C and 50 ± 5% relative humidity) with a constant deformation rate of 20 mm min^{-1} (the strain rate is 40%). The measurements were run three times for each sample and took the average value as the results.

2.4.8 Physicochemical properties

2.4.8.1 Thickness. The films thickness (mm) was measured, using a digital vernier caliper (Deli, China), at three different positions in each sample to the nearest 0.01 mm.

2.4.8.2 Water vapor transmission (WVT) and water vapor permeability (WVP). The water vapor transmission (WVT) and water vapor permeability (WVP) of films was determined by procedure for water method, using a modified ASTM E96/E96M-16-Standard Test Methods for Water Vapor Transmission of Materials. The obtained dry composite films were covered on the mouth of the cup and sealed by waterproof tape. The cup was filled with more than half of ultrapure water in order to generate 100% RH. Finally, the cup was placed in a desiccator filled with silica gel desiccant in order to provide 0% RH. The weight change of the cup was recorded every 12 hours, at room temperature (25 °C). Measure at least three times each time and take the average value to reduce errors. The water vapor permeability was calculated as follows:

$$\mathrm{WVT}\left(\mathrm{gm}^{-2}\ \mathrm{h}^{-1}\ \mathrm{mm}\right) = \frac{\Delta m \times X}{A \times t} \quad (1)$$

$$\mathrm{WVP}\left(\mathrm{gm}^{-2}\ \mathrm{h}^{-1}\ \mathrm{Pa}^{-1}\ \mathrm{mm}\right) = \frac{\mathrm{WVT}}{\Delta P} = \frac{\Delta m \times X}{A \times t \times P(R_1 - R_2)} \frac{1}{2} \quad (2)$$

where: Δm = the weight loss over time (g), X = the thickness of sample (mm), A = the test area or cup mouth area (m^2), t = the time (h), ΔP = the partial vapor pressure difference of the atmosphere with silica gel and pure water (Pa), P = the saturation vapor pressure at test temperature (3.169×10^3 Pa, 25 °C), R_1 = the relative humidity at test cup (100% RH), R_2 = the relative humidity at desiccator (0% RH).

2.4.8.3 Water vapor adsorption capacity and water resistance. The obtained dry composite films were conditioned at room temperature (25 °C) in desiccators for at least two weeks at 68.9% relative humidity for further analysis. The relative humidity is controlled by the saturated aqueous solution of KI. It has been verified that the humidity of the air above the liquid level of the saturated aqueous solution of KI in a closed container is about 68.9%. The water vapor adsorption capacity was test after the samples reached equilibrium state.

Moreover, the obtained dry composite films were immersed in ultrapure water for 12 hours. The water resistance was measured by characterizing its swelling behavior.

3. Results and discussion

3.1 Scanning electron microscopy (SEM)

The surface morphology of composite films with various SDS concentrations was shown in Fig. S2.† It is seen that the chitosan/SDS composite films are still able to maintain a flat and homogeneous microstructure, at a magnification of 5000×. All the films show no cracks, holes or other defects and have a similar surface appearance. This result suggests the presence of strong intermolecular interactions and superior compatibility between chitosan and SDS molecules.[18] We will further elaborate the mechanism of these interactions in the subsequent study.

3.2 Water vapor permeability (WVP)

Water vapor permeability (WVP) is an important parameter for food packaging materials, which can regulate the water vapor transmission effect between the food and the environment, and thus plays a role in preservation of food.[26,27] The WVP curves of samples were displayed in Fig. 1, and the result was shown in Table 1. The WVP of pure chitosan film was 1.7702 $gm^{-2}\ h^{-1}\ Pa^{-1}$ mm × 10^{-3}. And after cross-linked, the WVP of composite films was gradually reduced. This may be due to the intermolecular interactions of pure chitosan are dominated by hydrogen bonds, which are not tight, and the amount of water vapor allowed to pass through is relatively large. At the same time, the existence of hydrophilic groups (amino and hydroxyl groups) also contributes to the high WVP. For the composite films, the decrease of WVP is attributed to the presence of electrostatic interactions between chitosan and SDS, which reduces the amount of free hydrophilic groups on the polymer chains and makes the film structure more compact, resulting in low WVP.

3.3 Water vapor adsorption capacity and water resistance

The water vapor adsorption capacity of samples were determined and the result was shown in Table 1. It is seen that the pure chitosan film has the highest water content of about 18%. This result was well consistent with the early report by Agrawal that the moisture content was 19% for the hydrated chitosan film conditioned at relative humidity of 50%.[28] With the introduction of SDS, the water vapor adsorption capacity of composite films decreased gradually with the increase of the SDS concentration. For example, the water content of the composite film decreased from 15% to 12% when the SDS concentration increased from 1% to 12%. With further increasing SDS concentration, the water content leveled off and reached an equilibrium. When the SDS concentration is low, the binding sites formed by electrostatic interaction of $-SO_4^-$ with

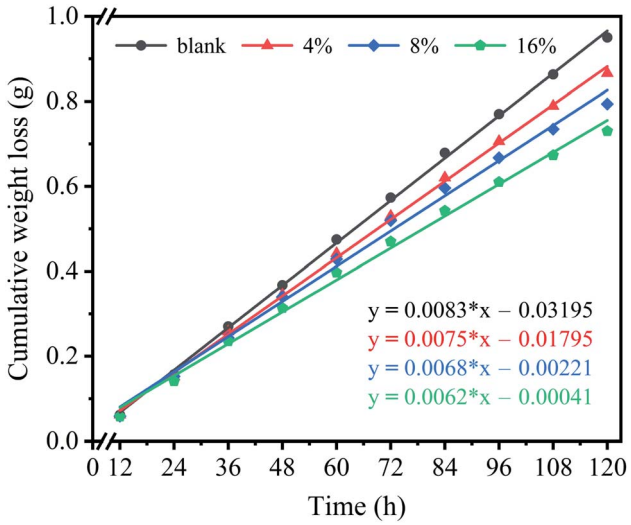

Fig. 1 The water vapor permeability curves of composite films with various SDS concentrations.

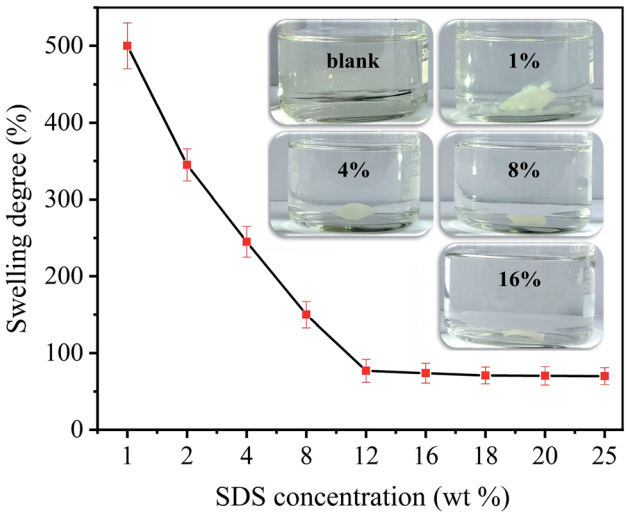

Fig. 2 Effect of SDS concentration on the swelling degree of composite films. The inset shows the photograph of composite films with various SDS concentrations swelled in water.

$-NH_3^+$ are very few due to low content of head groups. As the concentration of SDS increased, the binding sites of $-SO_4^-$ with $-NH_3^+$ gradually increased, and the number of hydrophilic groups ($-NH_3^+$) decreased, resulting in a low water vapor absorption capacity. When the SDS concentration reached a certain range, this binding was saturated, and the content of hydrophilic groups would not be further reduced.[29] Consequently, the water vapor absorption capacity of the composite films reached an equilibrium.

Generally, the chitosan film regenerated with acid solution can dissolve in water, and its water resistance is very poor.[6] Based on the results of water content of chitosan/SDS composite films, it is conjectured that the introduction of SDS may overcome this shortcoming. In order to further explore the effect of SDS on the water resistance of chitosan films, the swelling behavior of composite films were investigated, and the results were displayed in Fig. 2. Obviously, the cross-linking of chitosan films by SDS can significantly improve their water resistance.

As shown in the inset of Fig. 2, the composite films will not dissolve in water, and only swelled to a certain extent. Similar results have also been observed in other cross-linked chitosan film systems.[29] In this study, the ionic cross-linking neutralized the positive charges on the chitosan chains, leading to the fall of hydrophilic property.[11] In addition, with an increase in SDS concentration, the degree of swelling decreased and leveled off at 70%. This reduction of the swelling degree by ionic cross-linking has also been reported in chitosan/$CaCl_2$ system.[30] We attribute the decrease in the degree of swelling to the cross-linking between the $-SO_4^-$ anion and the $-NH_3^+$ ion. The degree of swelling decreases as the ionic cross-linking interaction increases. When all free $-NH_3^+$ groups are occupied, this anti-swelling effect reaches an equilibrium with the solubilization effect of water on chitosan. The degree of swelling does not decrease further. These findings indicate that the ionic cross-linking of chitosan by SDS can significantly enhance the hydrophobic properties, and improve the water resistance of biopolymer.

3.4 The interactions between chitosan and SDS

Fourier transform infrared spectroscopy (FTIR) was employed to study the interaction between chitosan and SDS and the results were shown in Fig. 3. For all samples, the broad absorption band at 3000–3600 cm^{-1} is caused by the superposition of the stretching vibration of the absorption peaks of $-NH_2$ and $-OH$, which can also be attributed to the large number of hydrogen bonds between chitosan molecules.[31] After being modified by SDS, this absorption peak became narrowed, and the intensity of the peak was also slightly reduced, indicating that the hydrogen bond between chitosan molecules was destroyed after cross-linked by SDS.[32] Additionally, it was stated that the decrease of the intensity of this peak corresponded to

Table 1 The WVT, WVP and water vapor adsorption capacity of various samples

Sample name	Thickness (mm)	WVT (gm^{-2} h^{-1} mm)	WVP (gm^{-2} h^{-1} Pa^{-1} mm × 10^{-3})	Water vapor adsorption capacity (%)
Blank	0.15 ± 0.01	5.6098	1.7702	18
4%	0.16 ± 0.01	5.0691	1.5996	14
8%	0.16 ± 0.01	4.5960	1.4503	12.5
16%	0.17 ± 0.01	4.4698	1.4105	12

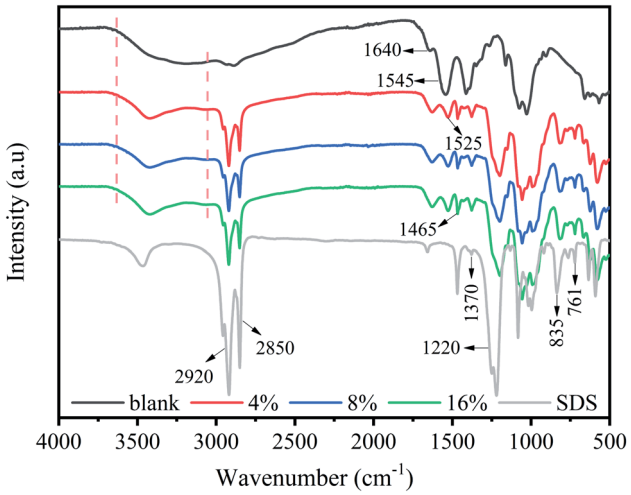

Fig. 3 FTIR spectra of composite films with various SDS concentrations.

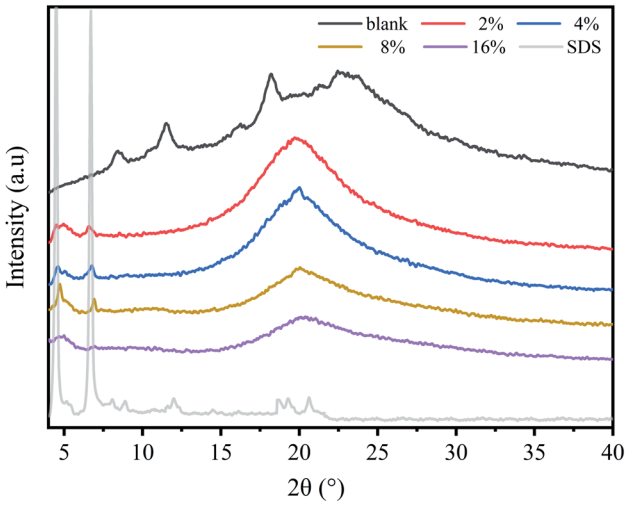

Fig. 4 XRD patterns of composite films with various SDS concentrations.

the reduction of the hydrophilicity.[33] The peaks appeared at 2900 cm^{-1} and 2850 cm^{-1} belong to the stretching vibration peak of CH_2, respectively. The reason is that after SDS addition, more CH_2 groups presented in the system, so the intensity of the two peaks was enhanced. The peaks at 1640 cm^{-1} and 1545 cm^{-1} were assigned to the stretching vibration peak of C=O (amide I) and the bending vibration peak of N–H (amide II), respectively.[23] The peaks at 1465 and 1370 cm^{-1} (the asymmetrical stretching vibrations of –C–O–S), 1220 cm^{-1} (S=O stretching vibration), 835 cm^{-1} and 761 cm^{-1} (the symmetric stretching vibration peaks of –S–O) were the characteristic signals of SDS,[11,34] which indicated the combination of SDS with chitosan.

Compared with the standard N–H bending vibration peak at 1582 cm^{-1}, this N–H peak (amide II) has shifted to the low wave number region at 1545 cm^{-1}. This is because the $-NH_2$ group in chitosan is protonated by H^+ into $-NH_3^+$, and the bending vibration of N–H is weakened.[35] In the chitosan/SDS composite films, this peak shifted from 1545 to 1525 cm^{-1}. The reason was that the free protonated $-NH_3^+$ could bind to $-SO_4^-$ anions through electrostatic interaction and form a neutral ion pairs, which shielded the original electrostatic repulsion between the chitosan chains. Similar result was observed in other chitosan/SDS systems.[23,24]

Based on the analysis of FTIR spectra, it was concluded that the addition of SDS weakened both the hydrogen bond and electrostatic interaction between chitosan molecules. Furthermore, it also induced a hydrophobic effect. Chitosan could be ionically cross-linked with SDS.

3.5 Crystalline structure of Chitosan/SDS composite films

In order to study the effect of SDS on the crystalline structure of chitosan films, the wide-angle X-ray diffraction patterns of composite films with different SDS concentrations were compared, and the results were shown in Fig. 4. It shows that three main diffraction peaks locate at $2\theta = 8.6°$, 11.5° and 18.3° for pure chitosan film. It is consistent with the diffraction spectrum of the hydration crystallization behavior of chitosan.[36] However, this result is different from previous study on the crystallization properties of acetic acid regenerated chitosan film.[37] It has been demonstrated that the crystallinity of chitosan film is closely related to the water content of polymer film, and the variation in the water content of the samples leads to the divergence of the results.[38]

For the composite films, only a broad scattering peak appears at $2\theta = 21°$, which indicates that the composite films have become the amorphous substance and the biopolymer chains were in amorphous state.[31] The reason may be that the addition of SDS anions destroys the ordered structure of the chitosan molecular chains due to the presence of interactions between SDS and biopolymer. The presence of this interaction can be confirmed by the shift in the position of the N–H peak (amide II) in the FTIR results (Fig. 3). Similar phenomenon has been reported by He *et al.*,[24] Furthermore, as the concentration of SDS increases, the intensity of the amorphous peak at $2\theta = 21°$ gradually decreases.

3.6 Energy spectrum and elemental analysis of chitosan/SDS composite films

To further confirm the combination of SDS with protonated chitosan, X-ray photoelectron spectroscopy (XPS) measurement was performed, and the results were shown in Fig. 5. The high resolution XPS spectra of S element for composite films is shown in Fig. S3 and S4.† It is seen that the characteristic signal of S 2p (168.3 eV) appears in the composite films, which confirms the existence of $-SO_4^-$ ion in the composite system after ion cross-linking. This result is in accordance with that of other studies.[24] In addition, the characteristic signal at 398.8 eV is attributed to $-NH_3^+$ ions (protonated amine) in the chitosan film,[24,39] and this signal has a red shift and the value moves to 400.9 eV in 6% composite film.[12] Furthermore, the signal intensity is also weakened after the introduction of SDS. In addition, the binding energy of N 1s is increased[21] and the number of protonated amines is decreased. The reason is that $-NH_3^+$ and $-SO_4^-$ in the system are combined through

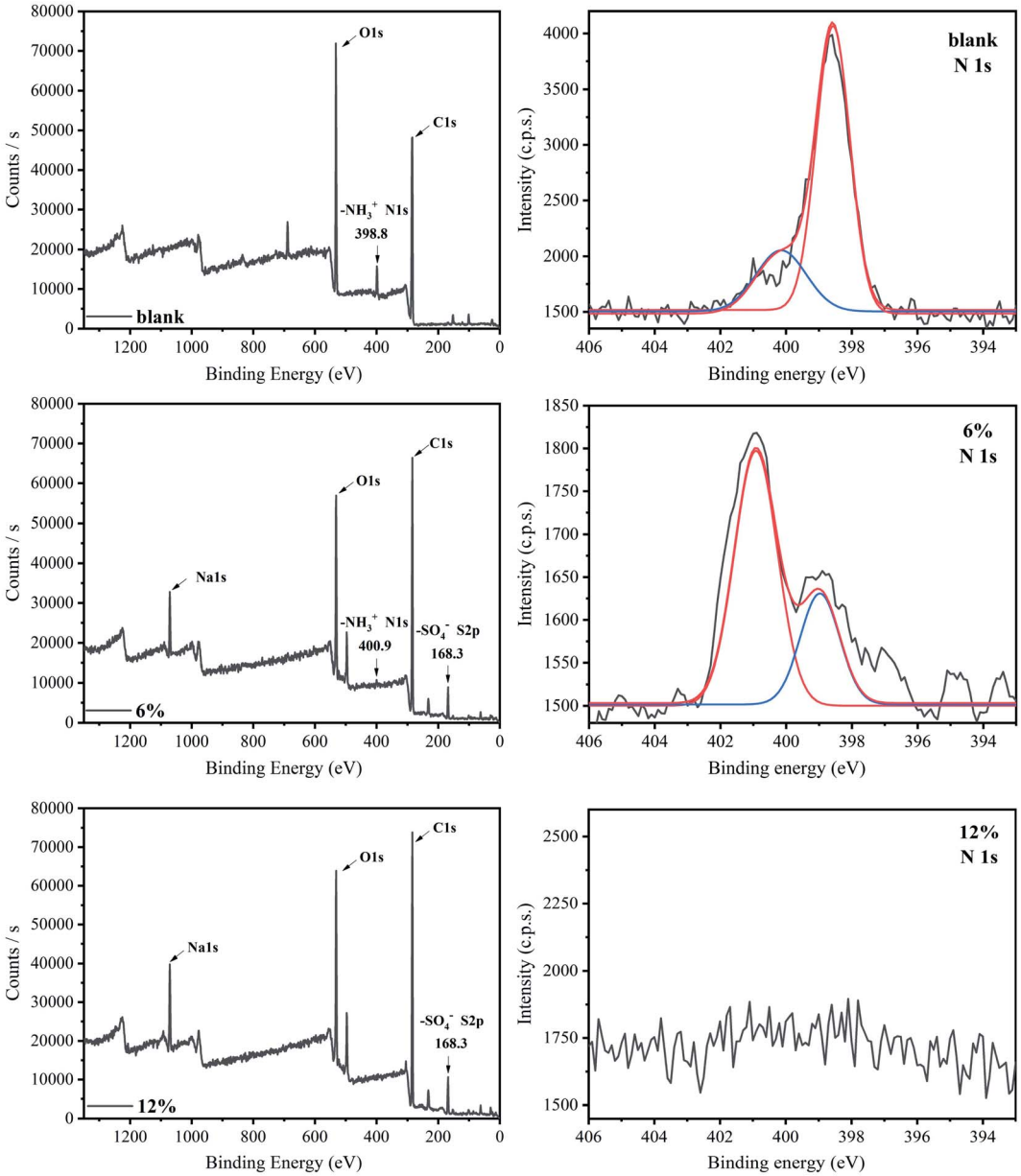

Fig. 5 XPS spectra of composite films with various SDS concentrations.

electrostatic interactions and become electrically neutral ion pairs. Accordingly, this characteristic signal is further reduced and disappears in 12% composite film. In this sample, all $-NH_3^+$ on the chitosan molecular chains and $-SO_4^-$ formed the neutral ion pairs, and the binding was saturated. These observations indicate that the binding of SDS to chitosan is through the interaction between $-NH_3^+$ and $-SO_4^-$, forming the ionic cross-linking in the composite films. Similar result was also reported in the SDS-chitosan hydrogel system.[24]

Fig. 6 displays the elemental analysis (EA) results. The pure chitosan sample contains approximately 3.6% of the N element and no S element. The composite films contain S element, which increases with increasing SDS concentration. When the SDS concentration is increased to 12 wt%, the content of S element no longer increases and reaches a stable level of 5.5%. In this study, the average molecular weight of chitosan sample is about 2.6×10^5,[38] and we can quantitatively analyze the interaction between $-NH_3^+$ (chitosan) and $-SO_4^-$ (SDS) through the ratio of N element to S element. It indicates that the molar ratio of $-NH_3^+$ cations to $-SO_4^-$ anions is about 1.5 : 1 in the chitosan/SDS composite film with saturated cross-linking. This ratio is different from previous result,[23] which can be attributed to the difference in the concentration of the solvent acid and the preparation process of chitosan films.

3.7 Thermal properties of chitosan/SDS composite films

In order to study the effect of SDS on the thermal properties of chitosan films, differential scanning calorimetry (DSC) tests

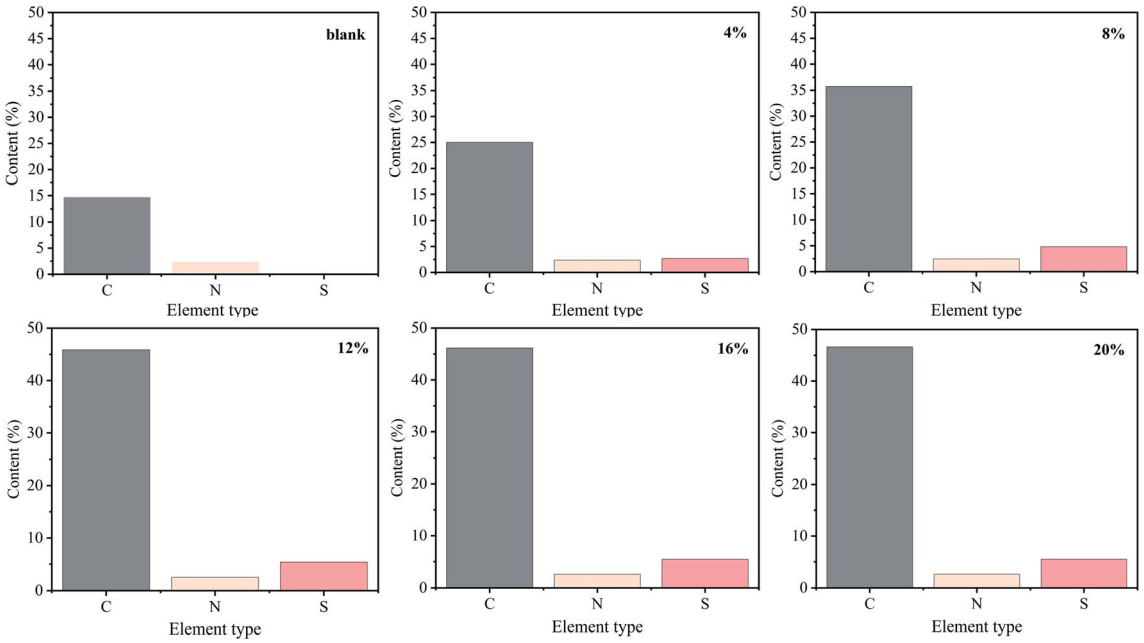

Fig. 6 EA results of composite films with various SDS concentrations.

were performed and the results were shown in Fig. 7. It is seen that the glass transition temperature (T_g) of the pure chitosan film is about 75 °C, which is different from the T_g values of chitosan reported in the literature.[38] However, the melting point of the pure chitosan film appears at about 105 °C, which is consistent with the conclusions has been reported by Qiao *et al.*[38] This difference may be due to the different water content of chitosan samples. It has been demonstrated that the T_g of chitosan depends on its moisture content due to the plasticizing effect of water molecules.[40] For the composite films, the T_g tends to increase with the increase of the SDS concentration, and finally reach about 107 °C for the 16% composite films. This is because SDS can cross-link the chitosan chains, and hinder the movement of the polymer chains, resulting in an increase of the glass transition temperature. Similar results have also been reported in the other cross-linked chitosan systems.[25,32] In addition, the elevation of T_g is also related to the reduction of the water content of the composite system, as confirmed by the TGA result (Fig. S1†). It has been generally accepted that the T_g of chitosan increased with the decrease of moisture content.[38]

Interestingly, an endothermic peak appeared in pure chitosan film, which can be attributed to the melting peak of the crystalline region of the chitosan film. This result is in good agreement with the XRD analysis that the crystalline regions exist in the chitosan film (Fig. 4). However, there is no endothermic peak in all the composite films, suggesting the chitosan chains are in amorphous state. In addition, there is only one transition process in the composite films, indicating that the ionic cross-link effect endows the SDS and chitosan with better cooperativity. This phenomenon of enhanced cooperativity was also observed in chitosan/SDS solutions.[18,25]

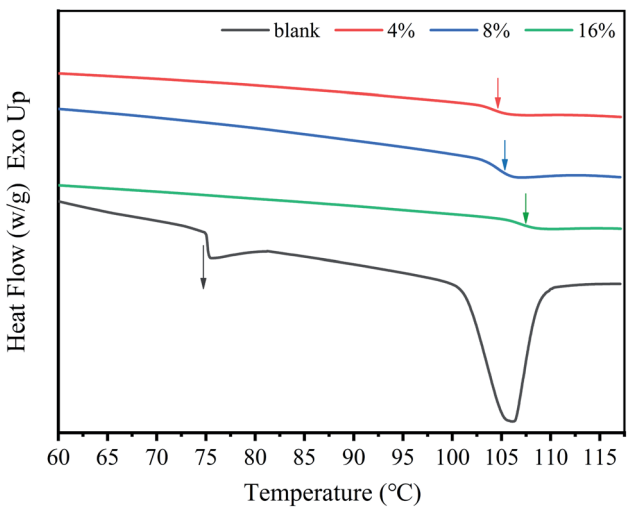

Fig. 7 DSC thermograms of composite films with various SDS concentrations.

The TGA curves of composite films with different SDS concentrations were shown in Fig. S5,† and the corresponding DTG thermograms were shown in Fig S6.† Generally, biological macromolecules have certain hygroscopicity. It can be seen from the TGA curves that the chitosan film has a relatively obvious weight loss stage before 150 °C, which corresponds to the removal of water. The introduction of SDS reduces the water content of the composite system, evidenced by the gentle weight loss platform for films with high SDS content. The weight loss stage between 200 to 400 °C corresponds to the decomposition of chitosan. This region corresponds to the decomposition of acetylated and deacetylated groups in chitosan.[41] Compared with the pure chitosan sample, the composite films have a notable weight loss at 260–400 °C. The high initial

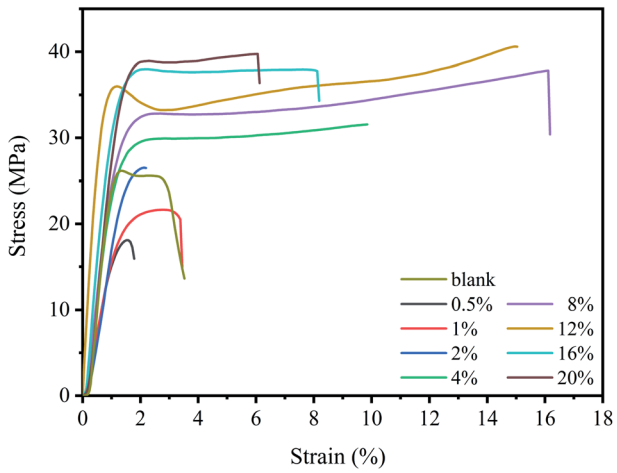

Fig. 8 The stress–strain curve of composite films with various SDS concentrations.

Table 2 The mechanical properties of composite films with various SDS concentrations

Mechanical parameters	Strength (MPa)	Elongation (%)	*E* (MPa)
Blank	26.2 ± 0.10	3.5 ± 0.04	20.2 ± 0.01
0.5%	18.1 ± 0.18	1.7 ± 0.02	10.3 ± 0.04
1%	20.5 ± 0.08	3.2 ± 0.06	11.4 ± 0.06
2%	26.5 ± 0.04	2.2 ± 0.04	12.6 ± 0.12
4%	28.5 ± 0.24	9.8 ± 0.06	17.8 ± 0.08
8%	32.8 ± 0.12	16.1 ± 0.12	23.9 ± 0.05
12%	39.9 ± 0.08	15.2 ± 0.10	32.6 ± 0.18
16%	38.1 ± 0.16	8.0 ± 0.08	32.3 ± 0.09
20%	39.1 ± 0.32	6.2 ± 0.12	27.2 ± 0.34

decomposition temperature is due to the formation of cross-link interactions between the SDS anions and the chitosan molecular chains, which inhibits the decomposition of chitosan.[33] The weight loss of various samples at different temperature stages was shown in Table S1.† These results show that the introduction of SDS improves the thermal stability of chitosan films at medium to high temperature.

3.8 Mechanical properties of chitosan/SDS composite films

Fig. 8 showed the stress–strain curves of composite films with different SDS concentrations at room temperature, and the result was shown in Table 2. It can be found that the pure chitosan film has poor mechanical properties with low elongation at break. It is known that there are a large number of hydrogen bonds in chitosan system and the polymer chain is rigid. Furthermore, the presence of crystalline regions also endows biopolymer with poor toughness.

SDS has a significant impact on the mechanical properties of the polymer films. When the concentration of SDS is low (~2%), the mechanical properties of the composite films became poor. At low SDS concentration, the cross-linking between $-SO_4^-$ ions and $-NH_3^+$ ions seldom occurred (Scheme 1). More important, a large number of free hydrophilic $-NH_3^+$ ions can interact with water, and tend to dissolve part of the film during the soaking of polymer film, which damages its mechanical properties.

With further increase of SDS concentration, both the strength and toughness were significantly enhanced,[24] and the best mechanical properties was achieved for 12% composite film with tensile strength of 40 MPa and elongation at break of 15%. These results indicate that a stable cross-linking network is formed by chitosan and SDS (Scheme 1), which can effectively inhibit the slip between chitosan chains when subjected to tension.[42]

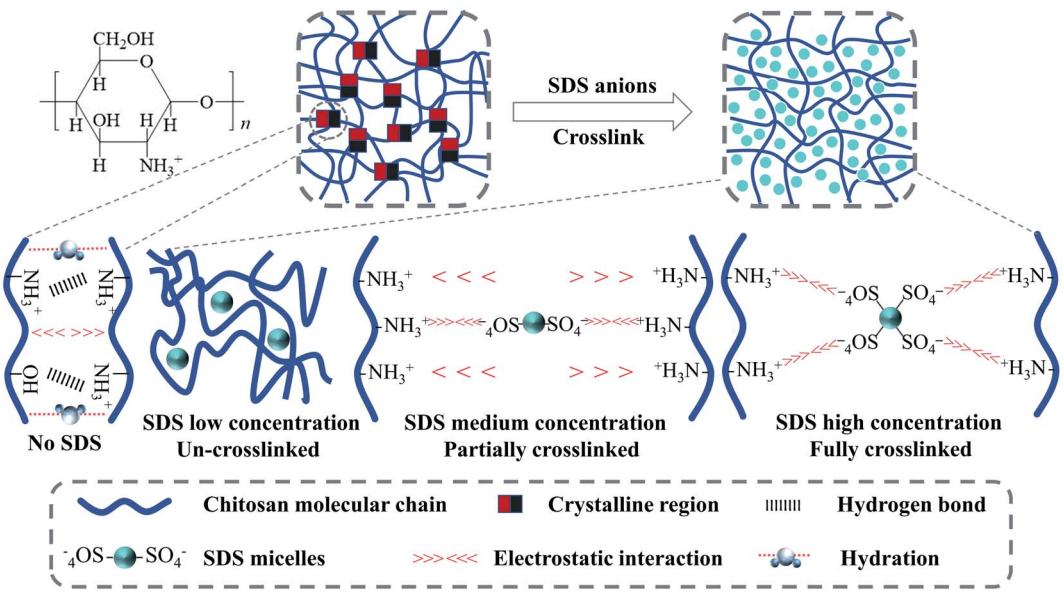

Scheme 1 The chitosan film regenerated from acetic acid has a certain crystallinity and hydration, which are weakened by the cross-link effect of SDS. This effect gradually increases with SDS concentration, until it is saturated.

However, when the SDS concentration is above 12%, the elongation at break of films decreases. At such high SDS concentration, the cross-linking of SDS will take a dominant position and produce an excessive cross-link effect.[43] This effect makes the rigidity of the chitosan chains become high, endowing the composite films hard and brittle, thereby impairing their mechanical properties. Similar results have been reported by,[43,44] who stated that the excessive number of cross-link points endowed the interaction between the polymer chains too strong and made the polymer with poor toughness.

In summary, the mechanical properties of composite films depend on SDS concentration. At low SDS content, few SDS micelles are embedded in chitosan chains and the cross-linking seldom occurs, resulting in poor mechanical properties. At moderate SDS content, a stable cross-linking system is formed and the mechanical properties are significantly improved. At high SDS content, the toughness is decreased due to the high degree of cross-linking.

4. Conclusions

SDS could bind strongly to chitosan through the interactions between $-SO_4^-$ and $-NH_3^+$ and formed an ionically cross-linked chitosan film. With an increase in SDS content, the moisture content of composite films decreased, and the crystallization of chitosan was seriously hindered and the biopolymer chains were in amorphous state. Due to the cross-linked effect the glass transition temperature of composite films increased. A melting peak appeared in the DSC traces for the chitosan film, whereas it was absent in composite films. Compared to pure chitosan film, the composite films possessed good thermal stability. In addition, the mechanical properties of composite films were closely related to the content of SDS. At low SDS content, the mechanical properties were poor. At moderate SDS content, both the tensile strength and toughness were significantly improved, while the toughness is decreased at high SDS content.

Author contributions

Song Jiang: conceptualization, data curation, formal analysis, investigation, methodology validation, visualization, writing – original draft, writing – review & editing. Congde Qiao: methodology, formal analysis, project administration, resources, supervision, writing – review & editing. Xujie Wang: investigation, writing–review & editing. Zhongwei Li: investigation, resources, writing – review & editing. Guihua Yang: resources, writing – review & editing.

Conflicts of interest

There are no conflicts to declare.

Acknowledgements

The work was supported by the Foundation (No. ZZ20190109) of State Key Laboratory of Biobased Material and Green Papermaking, Qilu University of Technology (Shandong Academy of Sciences).

References

1 L. Alison, A. F. Demirörs, E. Tervoort, A. Teleki, J. Vermant and A. R. Studart, *Langmuir*, 2018, **34**, 6147–6160.
2 M. Z. Elsabee and E. S. Abdou, *Mater. Sci. Eng. C*, 2013, **33**, 1819–1841.
3 M. G. N. Campos, L. H. I. Mei and A. R. Santos Jr, *Mater. Res.*, 2015, **18**, 781–790.
4 H. Wang, J. Qian and F. Ding, *J. Agric. Food Chem.*, 2018, **66**, 395–413.
5 N. E. Suyatma, L. Tighzert, A. Copinet and V. Coma, *J. Agric. Food Chem.*, 2005, **53**, 3950–3957.
6 C. Madeleine-Perdrillat, T. Karbowiak, F. Debeaufort, L. Delmotte, C. Vaulot and D. Champion, *Food Hydrocolloids*, 2016, **61**, 57–65.
7 P. Srinivasa, M. Ramesh, K. Kumar and R. Tharanathan, *J. Food Eng.*, 2004, **63**, 79–85.
8 T. Kato, M. Yokoyama and A. Takahashi, *Colloid Polym. Sci.*, 1978, **256**, 15–21.
9 H. Bao, L. Li, L. H. Gan and H. Zhang, *Macromolecules*, 2008, **41**, 9406–9412.
10 M. Thongngam and D. J. McClements, *J. Agric. Food Chem.*, 2004, **52**, 987–991.
11 S. Chatterjee, H. N. Tran, O.-B. Godfred and S. H. Woo, *ACS Sustainable Chem. Eng.*, 2018, **6**, 3604–3614.
12 X. Du, C. Kishima, H. Zhang, N. Miyamoto and N. Kano, *Appl. Sci.*, 2020, **10**, 4745.
13 D. Das and A. Pal, *Chem. Eng. J.*, 2016, **290**, 371–380.
14 C. Lin, S. Wang, H. Sun and R. Jiang, *J. Dispersion Sci. Technol.*, 2018, **39**, 106–115.
15 S. R. Bandforuzi and M. R. Hadjmohammadi, *Anal. Chim. Acta*, 2019, **1078**, 90–100.
16 X. Ren and Y. Zhang, *Colloids Surf., A*, 2020, **587**, 124316.
17 J. Grant, H. Lee, R. C. Liu and C. Allen, *Biomacromolecules*, 2008, **9**, 2146–2152.
18 R. Barreiro-Iglesias, C. Alvarez-Lorenzo and A. Concheiro, *J. Therm. Anal. Calorim.*, 2005, **82**, 499–505.
19 L. Chiappisi, I. Hoffmann and M. Gradzielski, *Soft Matter*, 2013, **9**, 3896–3909.
20 M. Thongngam and D. J. McClements, *Langmuir*, 2005, **21**, 79–86.
21 A. Dėdinaitė and M. Ernstsson, *J. Phys. Chem. B*, 2003, **107**, 8181–8188.
22 M. Lundin, L. Macakova, A. Dedinaite and P. Claesson, *Langmuir*, 2008, **24**, 3814–3827.
23 H. He, X. Cao, H. Dong, T. Ma and G. F. Payne, *Adv. Funct. Mater.*, 2017, **27**, 1605665.
24 H. He, J. Li, X. Cao, C. Ruan, Q. Feng, H. Dong and G. F. Payne, *ACS Appl. Bio Mater.*, 2018, **1**, 1695–1704.
25 H. S. Bae and S. M. Hudson, *J. Polym. Sci., Part A: Polym. Chem.*, 1997, **35**, 3755–3765.
26 S. S. Narasagoudr, V. G. Hegde, R. B. Chougale, S. P. Masti, S. Vootla and R. B. Malabadi, *Food Hydrocolloids*, 2020, **109**, 106096.

27 R. Priyadarshi, B. Kumar and Y. S. Negi, *Carbohydr. Polym.*, 2018, **195**, 329–338.
28 A. M. Agrawal, R. V. Manek, W. M. Kolling and S. H. Neau, *J. Pharm. Sci.*, 2004, **93**, 1766–1779.
29 J. Ostrowska-Czubenko, M. Pieróg and M. Gierszewska-Drużyńska, *J. Appl. Polym. Sci.*, 2013, **130**, 1707–1715.
30 M. Mahmoud Nasef, E. A. El-Hefian, S. Saalah and A. H. Yahaya, *E-J. Chem.*, 2011, **8**, S409–S419.
31 M. Chen, T. Runge, L. Wang, R. Li, J. Feng, X.-L. Shu and Q.-S. Shi, *Carbohydr. Polym.*, 2018, **200**, 115–121.
32 J. Ostrowska-Czubenko and M. Gierszewska-Drużyńska, *Carbohydr. Polym.*, 2009, **77**, 590–598.
33 F. A. Tanjung, S. Husseinsyah, K. Hussin and A. Hassan, *Polym. Bull.*, 2016, **73**, 1427–1445.
34 B. Zhang, X. Yang, P. Li, C. Guo, X. Ren and J. Li, *Carbohydr. Polym.*, 2018, **183**, 240–245.
35 S. Phattanarudee, K. Chakvattanatham and S. Kiatkamjornwong, *Prog. Org. Coat.*, 2009, **64**, 405–418.
36 M. Fan, Q. Hu and K. Shen, *Carbohydr. Polym.*, 2009, **78**, 66–71.
37 Y. Zhong, X. Song and Y. Li, *Carbohydr. Polym.*, 2011, **84**, 335–342.
38 C. Qiao, X. Ma, J. Zhang and J. Yao, *Carbohydr. Polym.*, 2019, **206**, 602–608.
39 G. Lawrie, I. Keen, B. Drew, A. Chandler-Temple, L. Rintoul, P. Fredericks and L. Grøndahl, *Biomacromolecules*, 2007, **8**, 2533–2541.
40 X. Ma, C. Qiao, J. Zhang and J. Xu, *Int. J. Biol. Macromol.*, 2018, **119**, 1294–1297.
41 J. Khouri, A. Penlidis and C. Moresoli, *J. Appl. Polym. Sci.*, 2020, **137**, 48648.
42 Y.-F. Qian, K.-H. Zhang, F. Chen, Q.-F. Ke and X.-M. Mo, *J. Biomater. Sci., Polym. Ed.*, 2011, **22**, 1099–1113.
43 T. Wang, X. Ren, Y. Bai, L. Liu and G. Wu, *Carbohydr. Polym.*, 2021, **254**, 117298.
44 M. P. Sokolova, M. A. Smirnov, A. A. Samarov, N. V. Bobrova, V. K. Vorobiov, E. N. Popova, E. Filippova, P. Geydt, E. Lahderanta and A. M. Toikka, *Carbohydr. Polym.*, 2018, **197**, 548–557.